Available online at www.sciencedirect.com
ScienceDirect
Applied Catalysis A: General 316 (2007) 117–124
APPLIED CATALYSIS A: GENERAL
www.elsevier.com/locate/apcata

A new catalyst material based on niobia/iron oxide composite on the oxidation of organic contaminants in water *via* heterogeneous Fenton mechanisms

L.C.A. Oliveira [a,*], M. Gonçalves [a], M.C. Guerreiro [a], T.C. Ramalho [a], J.D. Fabris [b], M.C. Pereira [b], K. Sapag [c]

[a] *Departamento de Química, Universidade Federal de Lavras, Caixa Postal 3037, CEP 37200-000 Lavras, Minas Gerais, Brazil*
[b] *Departamento de Química, Universidade Federal de Minas Gerais, Campus Pampulha, CEP 31270-901 Belo Horizonte, Minas Gerais, Brazil*
[c] *Departamento de Física, Laboratorio de Cs de Superfícies y Médios Porosos, Universidad Nacional de San Luis, Chacabuco 917, San Luis, Argentina*

Received 27 April 2006; received in revised form 17 September 2006; accepted 22 September 2006
Available online 7 November 2006

Abstract

The present work describes the preparation of novel materials based on niobia (Nb_2O_5)/iron oxides and their use as catalyst on oxidizing reactions of organic compounds in aqueous medium with hydrogen peroxide. These new composites were prepared by mixing natural niobia and iron oxides and were characterized with powder X-ray diffraction (XRD), chemical analyses, scanning electron microscopy (SEM), and ^{57}Fe Mössbauer spectroscopy. Results showed that the main iron oxides so formed were goethite (αFeOOH) and maghemite (γFe_2O_3) with small particle sizes. The decomposition study was realized with a basic dye as a model molecule: the methylene blue. The analysis of the products, with electrospray ionization mass spectrometry (ESI-MS), showed that the methylene blue was successively oxidized (hydrolyzed) through different intermediate species. These results strongly suggest that highly reactive hydroxyl radicals generated from the H_2O_2 on the surface of the 1:1 niobia:iron oxide composite act as an efficient heterogeneous Fenton catalyst

Keywords: Oxidation; Heterogeneous Fenton; Iron oxides; Hydrogen peroxide

1. Introduction

The Fenton reaction ($Fe^{2+} + H_2O_2 \rightarrow Fe^{3+} + {}^{-}OH + {}^{\bullet}OH$), involving hydrogen peroxide and Fe^{2+} in solution, is used to degrade contaminants, such as textile dyes, present in industrial waste waters [1]. In order to minimize the amount of the forming ferric hydroxide sludge in this homogeneous reaction [2], some iron oxides such as magnetite (ideal formula, Fe_3O_4), hematite (αFe_2O_3), goethite (αFeOOH) or ferrihydrite ($Fe_5HO_8{\cdot}4H_2O$), have been used instead of Fe^{2+} solutions [3–5]. The active heterogeneous redox processes are increasingly replacing the homogeneous systems in the catalysis research [6,7] and in some technological applications, such as in environmental remediation, as the solid species are easier to be removed from the reaction medium, being more easily recycled. In some cases, solid catalysts present better catalytic performance than their homogeneous counterparts do.

Many other important materials have been used as catalyst supports or promoters, but this work is particularly focused on niobia, for its natural occurrence and for the relatively high abundance of niobium in the Earth crust, which is about 20 ppm, in mass. Distributed by country, Brazil is the main niobium-supplier, providing about 60% of the world production. Despite of the increasing interest on their application in many technological fields, the niobium chemistry is not as deeply dominated as for other commonly used industrial metals in heterogeneous catalysis [8]. Niobium-based catalysts are effective in numerous reactions, including pollution control,

* Corresponding author. Tel.: +55 35 3829 1626.
E-mail address: luizoliveira@ufla.br (L.C.A. Oliveira).

0926-860X/$ – see front matter © 2006 Elsevier B.V. All rights reserved.
doi:10.1016/j.apcata.2006.09.027

selective oxidation, hydrogenation and dehydrogenation, dehydration and hydration, photochemistry, electrochemistry and polymerization. A remarkable application of niobium-based compounds is on oxidation catalysis.

The main purpose of this work was to prepare a new class of material based on a natural niobium oxide (Nb_2O_5 or simply niobia) and iron oxides to act as catalyst on the dye oxidation through a Fenton-like mechanism.

2. Materials and methods

2.1. Materials and characterization

The composites were prepared from a suspension of highly graded niobia (CBMM-Companhia Brasileira de Metalurgia e Mineração, Araxá-MG) in a 400 mL solution of $FeCl_3$ (7.8 g, 28 mmol) and $FeSO_4$ (3.9 g, 14 mmol) at 70° C. About 30 mL of a 5.0 mol L^{-1} NaOH solution was added drop-wise, in order to precipitate the iron oxides on the niobia surface. The materials were washed with distilled water until neutral pH. The amount of niobia was enough to obtain niobia:iron oxide mass ratios of 1:1 and 1:5. The obtained materials were dried at 105 °C for 3 h and characterized by powder XRD (Ni filtered Co Kα radiation, $\gamma = 0.17889$ nm); room temperature Mössbauer spectroscopy (^{57}Co/Rh source; isomer shifts are quoted relative to the αFe) and scanning electron microscopy (SEM) (Jeol-JKA 8900RL with Au sputtering coated samples fixed in a carbon tape).

2.2. The oxidative reactions

Three reactions took place in presence of the composite, according to the substrate: (i) the H_2O_2 decomposition to O_2 in water, (ii) the H_2O_2 decomposition to O_2 in presence of organic compounds and (iii) the oxidation of the dye methylene blue. The former, a typical decomposition of hydrogen peroxide, was carried out with 2 mL of H_2O_2 solution (30% v/v) in 5 mL of water and 30 mg of the composite. The mixture was stirred with a magnetic rod stirrer and the reaction was monitored by measuring the formation of gaseous O_2 in a volumetric glass system. The H_2O_2 decomposition in presence of organic compounds was carried out by using 5 mL solutions of 50 mg L^{-1} methylene blue, phenol and 2 mL of H_2O_2 solution with 30 mg of the composite. Finally, the activity of 30 mg of the composite in presence of hydrogen peroxide was tested in their effectiveness on discoloring 10 mL of methylene blue, taken from a 100 mg L^{-1} stock solution. The dye decomposition was monitored by measuring at 665 nm with a UV/Vis spectrophotometer Shimadzu UVPC 1600, all reactions at 25° C.

2.3. Studies by ESI-MS

In an attempt to identify the intermediate formation, the methylene blue decomposition was also monitored with the positive ion mode ESI-MS of an Agilent MS-ion trap mass spectrometer. The reaction samples were analyzed by introducing aliquots into the ESI source with a syringe pump at a flow rate of 5 μL min^{-1}. The spectra were obtained as an average of 50 scans of 0.2 s. Typical ESI conditions were as follows: heated capillary temperature 150° C; sheath gas (N_2) at a flow rate of 20 units (*ca.* 4 L min^{-1}); spray voltage 4 kV; capillary voltage 25 V; tube lens offset voltage 25 V. For ESI-MS/MS, the parent ion of interest was first isolated by applying an appropriate waveform across the end cap electrodes of the ion trap to resonantly eject all trapped ions, except those ions with *m/z* ratio of interest. The isolated ions were then subjected to a supplementary ac signal to resonantly excite them so to cause collision-induced dissociation (CID). The collision energy was set to a value at which ions were produced in measurable abundance.

All oxidation reactions or ion leaching were tested. The ion content in solution was tested by atomic absorption analysis, using a Varian AA 175 equipment.

2.4. Computational methods

The calculations were carried out with the package *Gaussian98* [9]. All transition states, intermediates and precursors involved were calculated. Each conformer was fully optimized by DFT [10]. The energy profile at selected DFT geometries along the reaction pathway were computed at the B3LYP level of theory by using the 6-31+G (d,p) basis set. For all different calculation methods, the algorithms based on conjugate gradient and quasi-Newton-Raphson were used for the geometry optimization, until reaching a gradient of 10^{-9} atomic units. The final geometries were obtained with DFT by using the Becke's three parameter hybrid functional with the LYP correlation functional [11] and density functional B3LYP using the basis set 6-311+G** [12]. This same computational procedure also elsewhere used for similar systems, with good results [13,14]. Furthermore, after each optimization, the nature of the stationary point was established by calculating and diagonalizing the Hessian matrix (force constant matrix). The unique imaginary frequency associated with the transition vector (TV) [15], *i.e.*, the eigenvector associated with the unique negative eigenvalue of the force constant matrix, was characterized. The solvent effect was evaluated with the polarized continuum model (PCM), initially proposed by Barone et al. [16], with the functional B3LYP and basis set 6-31+G(d,p). The solute cavity can then be specified as being any set of overlapping spheres. By representing the atoms as spheres, a more realistic cavity shape was produced for extended molecules, in contrast to another model of solvation [17].

3. Results and discussion

3.1. Hydrogen peroxide decomposition

Results of the hydrogen peroxide decomposition in presence of niobia/iron oxide composites are shown in Fig. 1. It is observed that the niobia:iron oxide 1:1 composite strongly favored the H_2O_2 decomposition. The pure iron oxide and

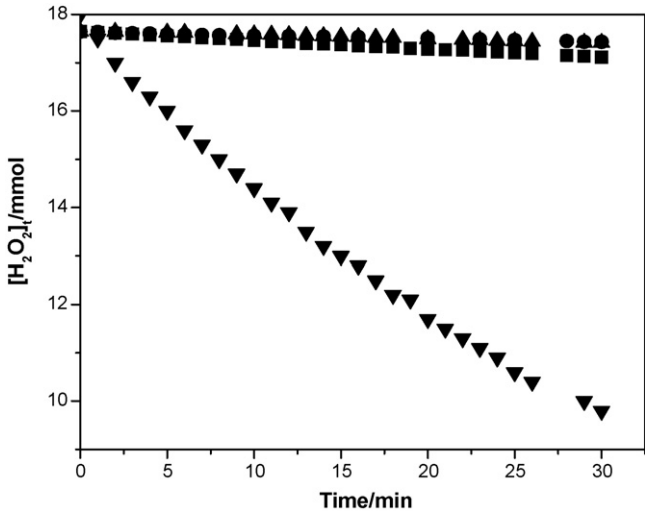

Fig. 1. Hydrogen peroxide decomposition in presence of the niobia:iron oxide composites.

niobia separately and the niobia:iron oxide 1:5 composite do not show any significant activity on the H_2O_2 decomposition. Fig. 2 shows results for the reaction in presence of phenol and drimaren red textile dye, for the niobia:iron oxide 1:1 sample. It can be observed that the H_2O_2 decomposition is strongly inhibited by the presence of the organic compounds. The reaction inhibition might be due to a competitive process involving the organic substrate and the active surface that could be related to (i) the adsorption of the organic compounds on the active sites of the composite and/or (ii) their reactions with intermediate species in the H_2O_2 decomposition reaction. Phenol is a radical scavenger and may be reacting with radical intermediates, such as $^{\bullet}OH$ or $^{\bullet}OOH$, species that are presumably formed during the H_2O_2 decomposition cycle [9–12]. The rate values of hydrogen peroxide consumption for the niobia:iron oxide 1:1 catalysts on organic oxidation are shown in Table 1.

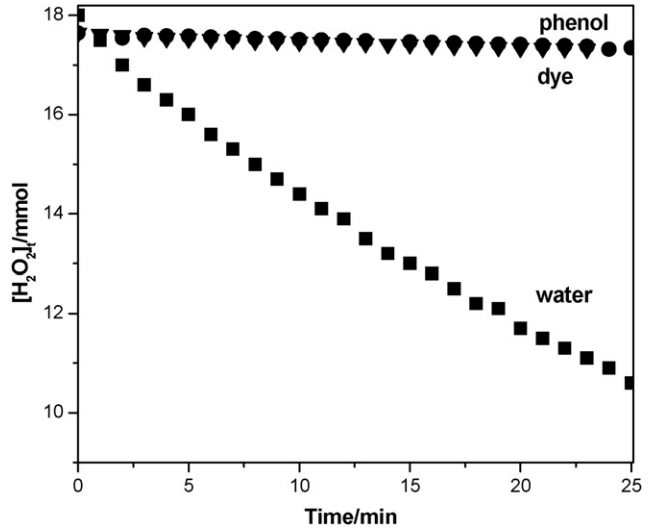

Fig. 2. Hydrogen peroxide decomposition in the presence of phenol and methylene blue using niobia:iron oxide 1:1 composite.

Table 1
Consumption rate (k) of hydrogen peroxide for the niobia:iron oxide 1:1 catalysts during substrate oxidation

Substrate	K ($\times 10^{-3}$ mol L^{-1} min^{-1})
Water	38.6 ± 0.1
Drimaren red dye	1.57 ± 0.03
Phenol	1.69 ± 0.02

3.2. Oxidation of the methylene blue dye

The oxidation of methylene blue with H_2O_2 in presence of the niobia:iron oxide composite was spectrophotometrically monitored through the discoloration of the solution (Fig. 3). It was observed that the concentration diminishes very slowly until 120 min. The pure niobia in presence of H_2O_2 showed the lower discoloring effect. The pure iron oxide and the composite with the highest iron content (niobia:iron oxide 1:5), in presence of hydrogen peroxide, showed similar discoloration efficiency, with approximately 50% of color removal. Differently, for the niobia:iron oxide 1:1 composite, the discoloration rate is highly increased. These results suggest that the composite is promoting the dye oxidation through a reaction pathway involving the peroxide.

The adsorption process and iron leaching were controlled by measuring the discoloration of the dye solution in a batch adsorption experiment, with the composites and the iron oxide (Fig. 4). Adsorption contributes with up to 15% to the discoloration process of the solution containing niobia:iron oxide 1:5. The iron content in solution, observed in the leaching test, was found to be very low, indicating that the discoloring reaction take place *via* a heterogeneous mechanism.

Control experiments with the composite in absence of H_2O_2 were then carried out in an attempt to effectively evaluate the contribution of adsorption in the discoloration process.

The reactions of methylene blue with niobia:iron oxide 1:1 composite (the more efficient catalyst for the oxidation among those studied in this work) and hydrogen peroxide were monitored with a UV-Visible spectrometry. Results (Fig. 5)

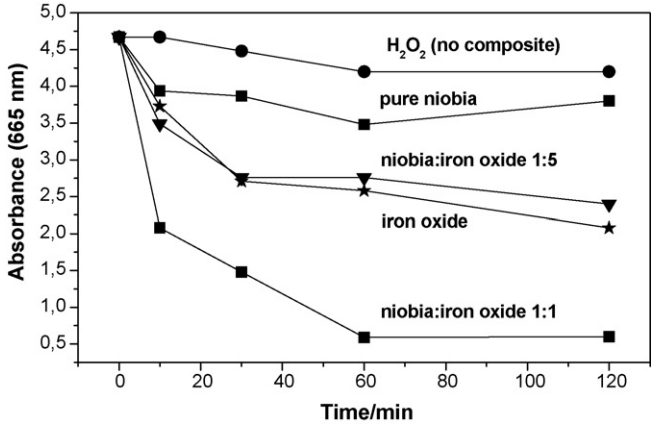

Fig. 3. Oxidation of methylene blue dye with H_2O_2 solely, and H_2O_2 in the presence of the pure iron oxide and niobia:iron oxide 1:1 composite.

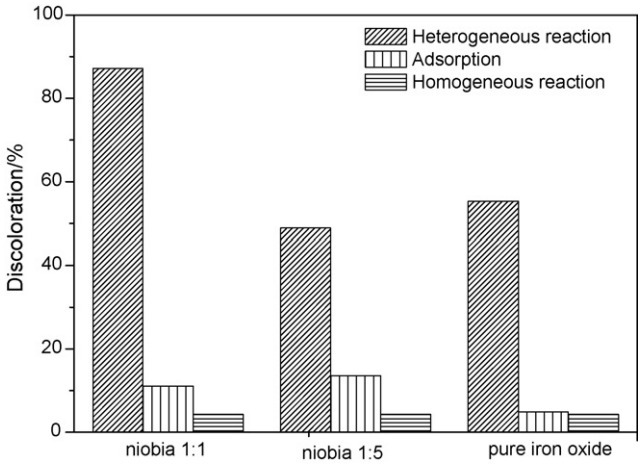

Fig. 4. Effect of the adsorption, homogeneous and heterogeneous oxidation in the discoloration of the methylene blue dye.

show a decreasing signal at 665 nm with the reaction time, following the discoloration of the solution with methylene blue dye. However, these results do not give any further clue about the nature of intermediates formed during the oxidation process. Besides the discoloration, it is interesting to discuss about the mineralization of organic dye. Even though the complete discoloration of methylene blue was observed to occur in less than 4 h reaction (Fig. 5) some intermediates may be being accumulated, which chemical species may also be environmentally harmful. Therefore, from the point of view of an industrial scale wastewater treatment, mineralization processes, in the sense to transform soluble organic intermediates to CO_2 and H_2O, is an issue to be taken into account. Actually it is more interesting to have a full mineralization than only a complete discoloration [13]. Results from the mass spectrometry analyses, applying the ESI for the screening of the oxidized species formed during the decomposition reaction of methylene blue with the niobia:iron oxide 1:1 composite and H_2O_2 system, are shown in Fig. 6. The ESI-MS spectrum

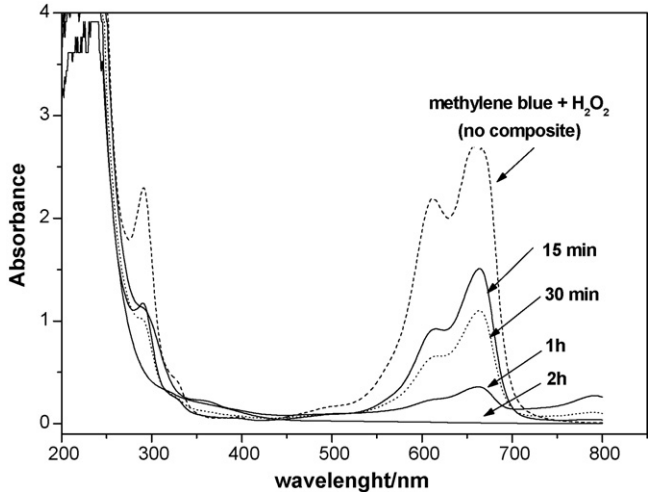

Fig. 5. Reactions of methylene blue dye with niobia:iron oxide 1:1 composite and hydrogen peroxide monitored by UV-Visible spectrometry.

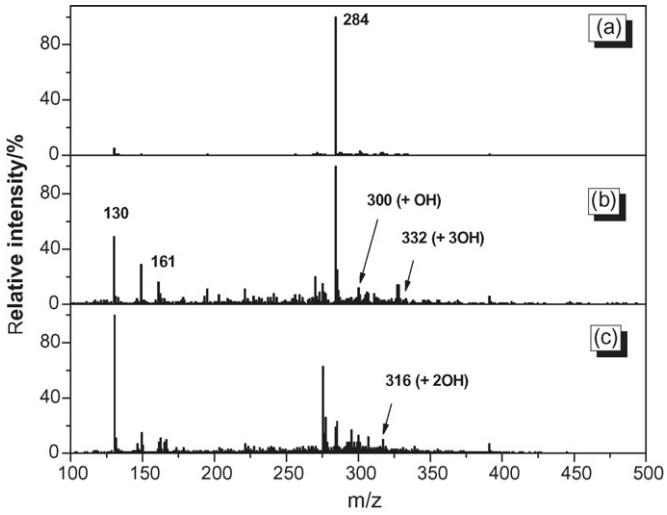

Fig. 6. ESI mass spectra in the positive ion mode for monitoring the oxidation of methylene blue dye in water by the niobia:iron oxide 1:1 and H_2O_2 system at different reactions times.

obtained for the dye solution shows only a strong signal at $m/z = 284$, which is related to the methylene blue ion (Fig. 6a). After 1 h reaction with the niobia:iron oxide 1:1 and hydrogen peroxide, a new m/z signals appears at 300 and 317, as shown in Fig. 6b. Fig. 6c show the ESI-MS spectrum for the reaction after 2 h. At this time, other m/z signals appear that are likely related to intermediates of the methylene blue oxidation, also suggesting that the structural ring is somehow broken apart. Fig. 7 shows the proposed intermediate structures of the complete oxidation reaction pathway, from methylene blue to CO_2 and H_2O.

3.3. Mössbauer spectroscopy, XRD and SEM

The room temperature Mössbauer spectra of composites and pure iron oxide are shown in Fig. 8. The whole spectra are formed by three sub spectra, each: two (super)paramagnetic doublets and one magnetic sextet. The complete assignment for all subspectral contributions from these complex data, which are thought to be due to the iron (hydr)oxides, is rather difficult, as resonance lines for the magnetic spectra are very broad. The sub-spectra relative to goethite were then fitted with a model-independent distribution of the hyperfine field (B_{hf}). Isomer shift values, for all samples, mentioned in Table 2 are characteristics of high spin Fe^{3+} in iron (hydr) oxides. From a qualitative analysis in Fig. 8, samples probably contain a complex mixture of poorly crystalline intermediate oxyhydroxide phases, which is shown in the distribution of the hyperfine field. The central doublets may eventually be due to species presenting superparamagnetic relaxation at room temperature, but no attempt was made at this stage to measure at lower temperatures to seek for a blocking transition.

The XRD analyses of the niobia/iron oxide composites and pure iron oxide (Fig. 9) show a cubic iron oxide phase ($d = 2.95$; 2.51; 2.09; 1.61; 1.48 Å), more likely related to the presence of maghemite, with lattice parameter of $a = 8.359$ Å, along with

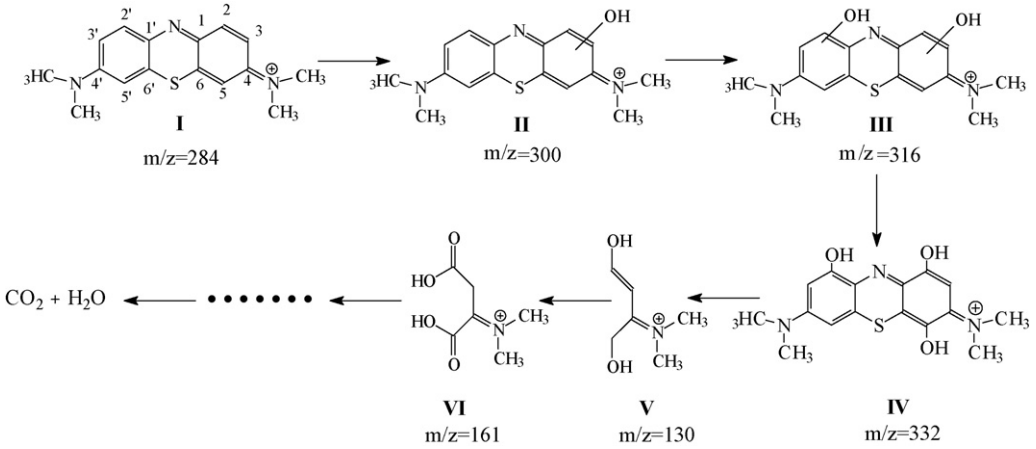

Fig. 7. Scheme with intermediates proposed for the oxidation of methylene blue dye ($m/z = 284$) by the niobia:iron oxide 1:1 and H_2O_2 system.

characteristic reflections assignable to goethite. It was not observed any diagnostic reflections for the pure niobia, implying its amorphous character. It is also interesting to observe that the niobia:iron oxide composite 1:1 present an XRD pattern of poorly crystalline material of iron oxide with highly dispersed niobia on its surface.

The SEM micrographs obtained for the niobia:iron oxide 1:1 composite, the pure niobia and the prepared iron oxide (Fig. 10a–d). Fig. 10a and b show the essential morphology of the prepared iron oxide aggregate and the original niobia [16]. A more general view of the composite can be observed in Fig. 10c and d. These images show details of the whole composite, the two materials appearing to have completely different textures: the niobia structure and the iron oxide aggregates are indicated by arrows.

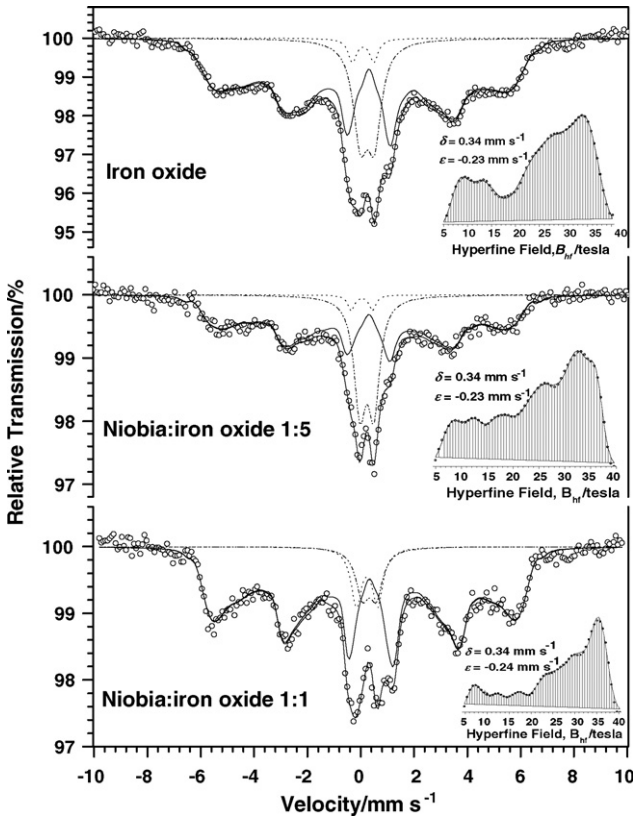

Fig. 8. Mössbauer spectra for the pure iron oxide and the niobia composites at room temperature.

3.4. Textural studies

Analyses by N_2 adsorption–desorption shows that the samples pure niobia, niobia:iron oxide 1:1 and niobia:iron oxide 1:5 present surface area of 72, 61 and 31 $m^2\,g^{-1}$, respectively. Moreover, values of microporous volume of 0.022, 0.019 and 0.018 $cm^3\,g^{-1}$ for pure niobia, niobia:iron oxide 1:1 and niobia:iron oxide 1:5, respectively, are affected by the influence of the iron oxide. These results suggest that the activity catalytic of the materials do not strongly affected by the surface area BET. The dispersion of the iron oxide seems to be an important characteristic of the composite.

3.5. Reaction mechanism

Although the hydrogen peroxide decomposition mechanism cannot be completely understood from these data, only. Several electron transfer processes are thought to take place during the reaction. According to the reportedly proposed mechanisms, the reaction initiates by an iron active site on the surface of the composite, with the H_2O_2 to produce a $^{\bullet}OH$ or by a process that involves the peroxide itself, by transferring an electron to an oxidizing site, yielding a $^{\bullet}OOH$ specie [17,18]. In the present case, both reactions, *i.e.* hydrogen peroxide decomposition and oxidation of organic compounds with H_2O_2 are likely to take place *via* radicals, as suggested by the inhibition effect observed during the H_2O_2 decomposition in the presence of organic compounds, such as phenol and methylene blue.

A simple competitive mechanism can alternatively be proposed for the hydrogen peroxide reactions in presence of the niobia composites. The reaction initiates by the activation of H_2O_2 through a Fenton-like mechanism [19] to produce an intermediate $^{\bullet}OH$ radical. This hydroxyl radical can then follow two competitive pathways: (i) either reacting with another H_2O_2 molecule leading to the auto-decomposition to O_2 or (ii)

Table 2
Fitted room temperature Mössbauer parameters for pure iron oxide and niobia composites (δ, isomer shift relative to αFe; ε, quadrupole shift, Δ, quadrupole splitting; B_{hf}, hyperfine field; Γ, sub-spectra middle height line width and RA, relative sub-spectral area)

Sample	Site ^{57}Fe	δ (mm s^{-1})	ε, Δ (mm s^{-1})	B_{hf} (T)	Γ (mm s^{-1})	RA (%)
Iron oxide	Goethite	0.341 (2)	−0.23	34.9 (6)[a]	0.31	78.1 (2)
	$^{VI}Fe^{3+}$	0.391 (7)	0.52		0.64 (4)	19.0 (2)
	$^{VI}Fe^{3+}$	0.23 (2)	0.80		0.39 (8)	2.9 (2)
Novia:iron oxide 1:5	Goethite	0.341 (2)	−0.23	36.19 (7)[a]	0.31	71.4 (2)
	$^{VI}Fe^{3+}$	0.374 (7)	0.52		0.52 (3)	26.3 (2)
	$^{VI}Fe^{3+}$	0.19 (3)	0.80		0.30	2.3 (2)
Niobia:iron oxide 1:1	Goethite	0.341 (2)	−0.24 (1)	35.7 (1)[a]	0.31	83.1 (2)
	$^{VI}Fe^{3+}$	0.42 (1)	0.52		0.59 (1)	8.4 (2)
	$^{VI}Fe^{3+}$	0.33 (1)	0.80		0.48 (7)	8.5 (2)

[a] Maximum hyperfine field of the distribution.

oxidizing organic compounds found in the aqueous medium. In order to shed some more light on this model of the overall reaction mechanism, it was performed calculations of the Gibbs free energy for the stability of the intermediates, by the algorithm implemented in the *Gaussian98* package [9]. All discussions concerning the energy differences and the energy barriers refer to the enthalpy term corrected for the zero point energy at 298.15 K. The resulting energies values are presented in Table 3 and Fig. 7. From this calculation, it was found a good agreement between the modeled and experimental geometry for the methylene blue molecule [20]. According to data listed in Table 3, it can be observed that the hydroxyl group on C2 position is about +3.30 and +6.65 kcal mol^{-1} more stable than the alternative C3 and C5, respectively. These results put in evidence that the preferential reaction site for •OH in this Fenton process is the position 2 (C2) of the methylene blue structure, resulting in an intense fragment corresponding to $m/z = 300$ (Fig. 7). Further calculations revealed that the hydroxylation occurs on C4 (see Table 3), which explains the resulting intense fragment corresponding to $m/z = 316$ (Fig. 7). Dyes are usually difficult to be bio-decomposed, although Fenton degradation and mineralization steps have been reportedly found for various dyes [21,22]. From these theoretical results, compounds **II** and **III** (Fig. 7) are supposed to be stables and can be experimentally detected, although no further attempt was made in this work to address this analysis. Moreover, the reaction path may still involve other hydroxylations. From these results, the third hydroxylation would more likely occur at 5′ position. This is crucial step, as it would simultaneously lead to the formation of hydroquinone or hydroquinone-like intermediates generated by the •OH attack. A reaction mechanism was earlier proposed for the interaction between Fenton reagents or aromatic compounds [23] and Orange II dye [24], which involves the generation of hydroquinone or hydroquinone-like and the redox cycle of hydroquinone/quinone in the Fenton reaction. That is an unstable key-intermediate that points out the quick and high probability of rupture of both chemical bonds C1–C2 and C5–C6 (Fig. 5). This could justify the formation of **V** ($m/z = 130$). It should also be noted that the degradation of methylene blue exhibits an induction period at the begging of the reaction (Fig. 6), which suggests that some degradation intermediates play an important role to promote the Fenton reaction. Nevertheless, the presence of •OH in the reaction medium, the oxidation of **V** probably occurs, which consequently generates the stable specie **VI**, with $m/z = 161$. These calculations show a good agreement with experimental data (Fig. 7). To date, no other similar theoretical study devoted to investigate the degradation mechanism *via* heterogeneous Fenton of the methylene blue has been reported. Further and still more accurate theoretical calculations in order to verify this hypothesis are now in progress.

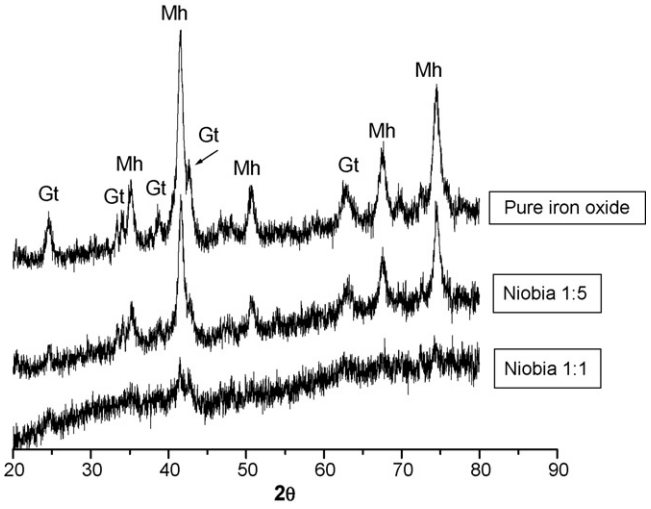

Fig. 9. XRD of pure iron oxide and niobia composites.

Table 3
Gibbs free energy of **II** and **III** intermediates using B3LYP/6-31+G(d,p)

Intermediate	Hydroxyl position	ΔG (kcal mol^{-1})
II	2	0.00
	3	+3.30
	5	+6.04
III	2, 2′	0.00
	2, 5′	+34.69
	3, 2′	+11.73
	3, 3′	+14.26
	3, 5′	+3.25
	5, 5′	+21.22

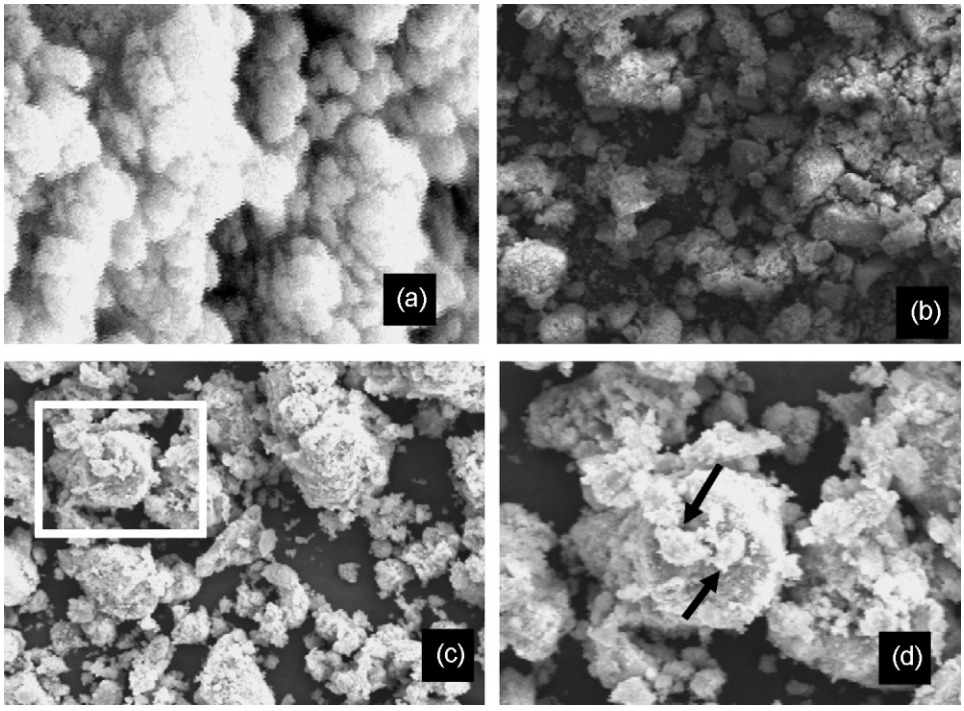

Fig. 10. SEM micrographs (scale = 1 μm) of (a) pure iron oxide, (b) pure niobia, (c) niobia 1/1 and (d) a detail of the composite.

4. Conclusion

Data from this work show that the chemical properties of niobia can strongly be modified when forming composites with iron (hydroxy) oxides. The resulting materials show a remarkable effect in discoloration an organic dye in aqueous medium. ESI-MS studies of the methylene blue oxidation showed the hydroxylation until CO_2 is ultimately formed, suggesting that it is possible to reach the total mineralization of the organic substrate; not only its discoloration. Preliminaries calculations of the Gibbs free energy at DFT level show a good accordance with experimental data, which could justify, in principle, the presence of the intense fragments founds at $m/z = 300$, 316, 161 and 130 in the mass spectra. The compound corresponding to $m/z = 332$ was found to be a very unstable chemical specie. The composites characterization, particularly with X-ray diffraction and Mössbauer spectroscopy, suggest the formation of an active phase of iron oxide on the surface of the natural niobia and that the iron oxide dispersion does occur on the niobia:iron oxide 1:1 more intensely than on niobia:iron oxide 1:5. This dispersion responds for the decomposition of H_2O_2 and of the dye. The decomposition of hydrogen peroxide takes place *via* a radical mechanism, probably initiated by an electron transfer from the active site, on the surface of the composite, to H_2O_2 to produce species such as $^{\bullet}OH$ or $^{\bullet}OOH$. The ESI-MS m/z signals account for the presence of intermediate structures in the reaction medium.

Acknowledgments

Work supported by CNPq and FAPEMIG (Brazil). Authors are indebted to Dr. Robson (CBMM) for providing the natural niobia samples and to Prof. Dr. C.A. Taft (CBPF) for the computation facilities.

References

[1] M. Lu, J. Chen, H. Huang, Chemosphere 46 (2002) 131–136.
[2] S. Chou, C. Huang, Chemosphere 38 (1999) 2719–2731.
[3] R.J. Watts, M.D. Udell, P.A. Rauch, S.W. Leung, Hazard. Waste Hazard. Mater. 7 (1990) 335–345.
[4] B.W. Tyre, J. Environ. Qual. 20 (1991) 832–838.
[5] W.P. Kwan, B.M. Voelker, Environ. Sci. Technol. 36 (2002) 1467–1476.
[6] I.W.C.E. Arends, R.A. Sheldon, Appl. Catal. A 212 (2001) 175–187.
[7] L. Menini, M.J. Silva, M.F.F. Lelis, J.D. Fabris, R.M. Lago, E.V. Gusevskaya, Appl. Catal. A 269 (2004) 117–121.
[8] I. Nowak, M. Ziolek, Chem. Rev. 99 (1999) 3603–3624.
[9] Gaussian 98, Revision A.9, M.J. Frisch, G.W. Trucks, H.B. Schlegel, G.E. Scuseria, M.A. Robb, J.R. Cheeseman, J.A. Montgomery Jr., T. Vreven, K.N. Kudin, J.C. Burant, J.M. Millam, S.S. Iyengar, J. Tomasi, V. Barone, B. Mennucci, M. Cossi, G. Scalmani, N. Rega, G.A. Petersson, H. Nakatsuji, M. Hada, M. Ehara, K. Toyota, R. Fukuda, J. Hasegawa, M. Ishida, T. Nakajima, Y. Honda, O. Kitao, H. Nakai, M. Klene, X. Li, J.E. Knox, H.P. Hratchian, J.B. Cross, V. Bakken, C. Adamo, J. Jaramillo, R. Gomperts, R.E. Stratmann, O. Yazyev, A.J. Austin, R. Cammi, C. Pomelli, J.W. Ochterski, P.Y. Ayala, K. Morokuma, G.A. Voth, P. Salvador, J.J. Dannenberg, V.G. Zakrzewski, S. Dapprich, A.D. Daniels, M.C. Strain, O. Farkas, D.K. Malick, A.D. Rabuck, K. Raghavachari, J.B. Foresman, J.V. Ortiz, Q. Cui, A.G. Baboul, S. Clifford, J. Cioslowski, B.B. Stefanov, G. Liu, A. Liashenko, P. Piskorz, I. Komaromi, R.L. Martin, D.J. Fox, T. Keith, M.A. Al-Laham, C.Y. Peng, A. Nanayakkara, M. Challacombe, P.M.W. Gill, B. Johnson, W. Chen, M.W. Wong, C. Gonzalez, J.A. Pople, Gaussian Inc., Wallingford CT, 1998.
[10] H.G. Li, G.K. Kim, C.K. Kim, S. Rhee, I. Lee, J. Am. Chem. Soc. 123 (2001) 2326.
[11] A.D. Becke, J. Chem. Phys. 98 (1993) 5648.
[12] S. El-Taher, R.H. Hilal, Int. J. Quantum Chem. 20 (2001) 242.
[13] T.C. Ramalho, M. Buhl, Magn. Reson. Chem. 43 (2005) 139–146.

[14] E.F.F. da Cunha, T.C. Ramalho, R.B. de Alencastro, C.A. Taft, Lett. Drug Des. Discov. 3 (2006) 625–632.
[15] J.W. McIver Jr., Acc. Chem. Res. 7 (1994) 72.
[16] V. Barone, M. Cossi, J.J. Tomasi, Comp. Chem. 19 (1998) 404–417.
[17] L.C.A. Oliveira, C.N. Silva, M.I. Yoshida, R.M. Lago, Carbon 42 (2004) 2279–2284.
[18] R.C.C. Costa, M.F. Lelis, L.C.A. Oliveira, C.N. Silva, R.M. Lago, Catal. Commun. 4 (2003) 525–529.
[19] V.R. Komandur, C.P. Kumara, A. Murali, A. Tripathi, A. Clearfield, J. Mol. Catal. A: Chem. 216 (2004) 139–146.
[20] I. Ma, W. Song, C. Chen, W. Ma, J. Zhao, Y. Tang, Environ. Sci. Technol. 39 (2005) 5810–5815.
[21] F. Chen, W. Ma, J. He, J. Zhao, J. Phys. Chem. A 106 (2002) 9485–9490.
[22] I.Y. Litvintev, Y.V. Mitnik, A.I. Mikhailyuk, S.V. Timofeev, V.N. Sapunov, Kinet. Catal. 34 (1993) 71–75.
[23] J. Bandeara, C. Marrison, J. Kiwi, J. Plugarin, P. Pevinger, J. Photochem. Photobiol. A: Chem. 99 (1996) 57.
[24] N.H. Ince, D.A. Hasan, B. Ustun, G. Tezcanli, Water Sci. Technol. 46 (2002) 51–58.